AD-A112 305 HUGHES AIRCRAFT CO EL SEGUNDO CA DISPLAY SYSTEMS LAB F/G 6/17
LASER EYE PROTECTION.(U)
JUL 79 K C JOHNSON, G E MOSS N62269-77-R-0307
UNCLASSIFIED HAC-E1562 NL

END
DATE FILMED
4 82
DTIC

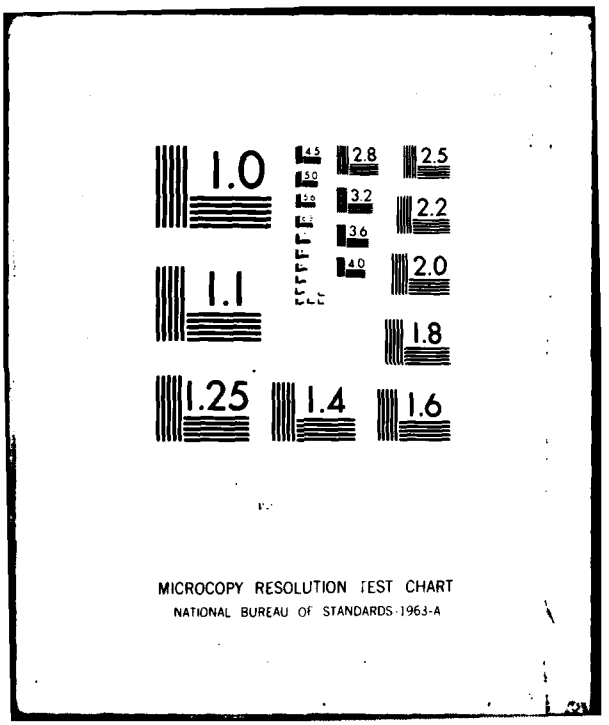
1.0
1.1
1.25
1.4
1.6
2.8
3.2
3.6
4.0
2.5
2.2
2.0
1.8
MICROCOPY RESOLUTION TEST CHART
NATIONAL BUREAU OF STANDARDS-1963-A

12

FINAL REPORT FOR PERIOD AUGUST 1977 TO JUNE 1979

LASER EYE PROTECTION

JULY 1979

PREPARED FOR: NAVAL AIR SYSTEMS COMMAND, DEPARTMENT OF THE NAVY

AEROSPACE GROUPS

HUGHES

HUGHES AIRCRAFT COMPANY
CULVER CITY CALIFORNIA

HAC REPORT NO. FR 79-27-996

SECURITY CLASSIFICATION OF THIS PAGE (When Data Entered)

REPORT DOCUMENTATION PAGE		READ INSTRUCTIONS BEFORE COMPLETING FORM
1. REPORT NUMBER	2. GOVT ACCESSION NO. AD-A112 305	3. RECIPIENT'S CATALOG NUMBER
4. TITLE (and Subtitle) Laser Eye Protection Purchase Description CSVL-04; Device, Laser Eye Protection		5. TYPE OF REPORT & PERIOD COVERED Final Technical Report 8/11/77 to 6/79 6. PERFORMING ORG. REPORT NUMBER E1562, FR 79-27-996
7. AUTHOR(s) Kenneth C. Johnson Gaylord E. Moss		8. CONTRACT OR GRANT NUMBER(s) N62269-77-R-0307
9. PERFORMING ORGANIZATION NAME AND ADDRESS Diffraction Optics Dept., Display Systems Lab., Engineering Division, Radar Systems Group, Hughes Aircraft Co., 2000 E. Imperial Hwy., El Segundo, Calif. 90009		10. PROGRAM ELEMENT, PROJECT, TASK AREA & WORK UNIT NUMBERS 62758N; F51-523; WF 51-523-401; ZB 104
11. CONTROLLING OFFICE NAME AND ADDRESS Naval Air Systems Command Department of the Navy Washington, D.C. 20361		12. REPORT DATE July 1979 13. NUMBER OF PAGES 36
14. MONITORING AGENCY NAME & ADDRESS(if different from Controlling Office) Crew Systems Department (code 40) Naval Air Development Center Warminster, PA 18974		15. SECURITY CLASS. (of this report) Unclassified 15a. DECLASSIFICATION/DOWNGRADING SCHEDULE
16. DISTRIBUTION STATEMENT (of this Report) Approved for public release; distribution unlimited.		
17. DISTRIBUTION STATEMENT (of the abstract entered in Block 20, if different from Report)		
18. SUPPLEMENTARY NOTES		
19. KEY WORDS (Continue on reverse side if necessary and identify by block number) Eye Protection Laser Filter		

20. ABSTRACT (Continue on reverse side if necessary and identify by block number)

A design for a narrow-band diffractive radiation shield to be fabricated on a helmet visor has been developed and tested. An experimental feasibility study indicates that 99.9% shielding of a specified laser wavelength may be achieved with a visor positioned on the order of 7 cm from the eye (Photopic transmittance is expected to exceed 90%.) Several technic obstacles remain to be overcome before a full-scale workable prototype can constructed, but shielding efficiencies far better than the 99.9% demonstrated value may become possible as the technology develops.

DD FORM 1 JAN 73 1473 EDITION OF 1 NOV 65 IS OBSOLETE

SECURITY CLASSIFICATION OF THIS PAGE (When Data Entered)

CONTENTS

LIST OF ILLUSTRATIONS

LIST OF ILLUSTRATIONS (Continued)

1.0 INTRODUCTION

This report covers work done on contract No. N62269-77-R-0307 at the Hughes Aircraft Company in Culver City, California between August 1977 and June 1979. Sponsorship was by the Naval Air Development Center at Warminster, Pennsylvania under the technical direction of Dr. Gloria Chisum.

2.0 SUMMARY

The objective of the Laser Eye Protection program has been to study and demonstrate the feasibility of applying diffraction optics techniques to the design of a protective visor which would shield its wearer from light at specified laser wavelengths. The most promising method examined, which would use two holographic diffraction gratings on a helmet visor, has been analyzed in detail and tested experimentally. One particular test sample exhibits measured transmission at 504 nm of less than 0.1 percent over an angular range of 24°, which would cover roughly a 30 mm diameter region of the eye with a visor positioned 70 mm in front of the eye. Measured photopic transmittance is 75 percent. (Of the light loss of 25 percent, only 9 percent is loss due to the hologram with the remainder being 9 percent inherent surface reflection and 7 percent glass absorption in the substrate. In an operational device the losses can be reduced to 9 percent by using antireflection coated clear substrates.) Although considerable further developmental work will be required to produce holographic gratings exhibiting these characteristics over large surface areas on curved plastic substrates with the necessary stability and uniformity, these preliminary results indicate that one can eventually achieve over 99.9 percent shielding of the eye region from a designated wavelength with an acceptable overall photopic transmittance of better than 90 percent.

3.0 DESIGN ALTERNATIVES

3.1 BANDPASS VERSUS BAND REJECTION

During the first phase of this program a number of alternative eye protection approaches were examined. These approaches fall into two general categories.

1. Bandpass type devices which transmit only certain selected safe bandwidths and reject all wavelengths outside those bands.
2. Band rejection type devices which reject only certain selected dangerous wavelengths and transmit all wavelengths outside the rejection bands.

Figure 1 and Figure 2 show the light transmission to the eye for each of these protection approaches. The bandpass type device has the advantage that the precise wavelength of protection need not be known but it has the

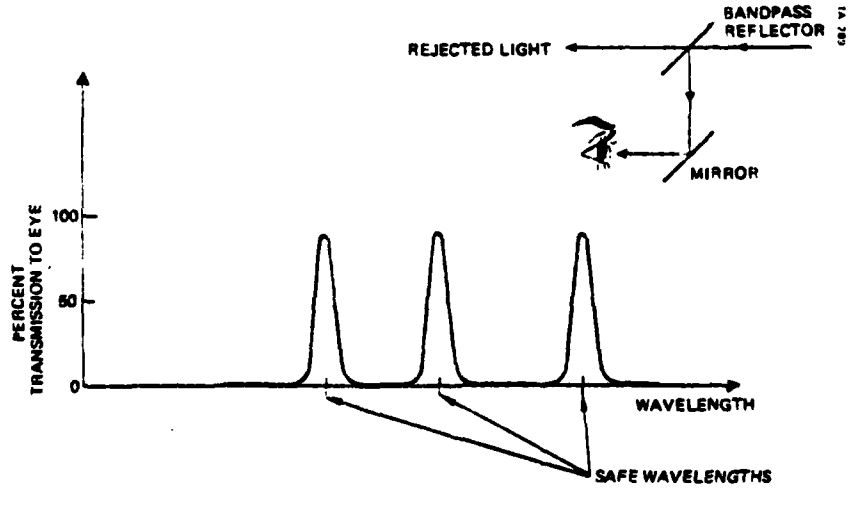

Figure 1. Bandpass type eye protection device.

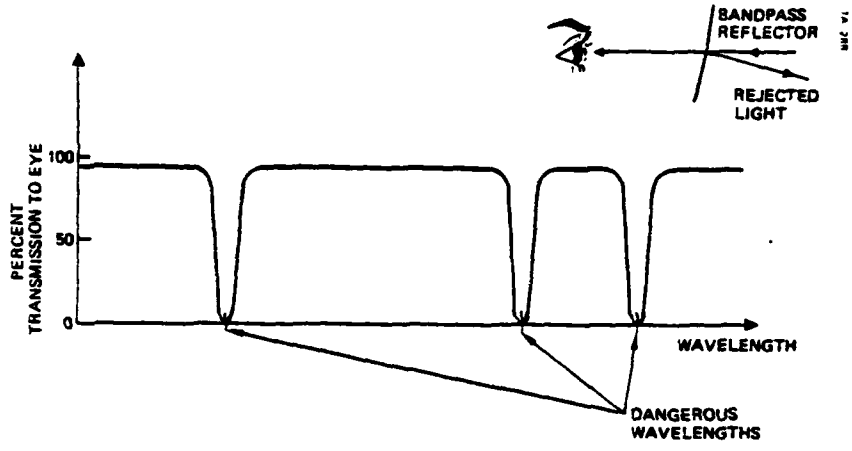

Figure 2. Band rejection and eye protection.

disadvantage that the view will be dim and colored because the viewer sees only in a narrow band or bands.

Another disadvantage is that the bandpass type methods that were considered incorporate either periscope-like selective mirror configurations or selective transmission lens arrangements that are incompatible with a conventional visor. Because the immediate problem is to protect against only one or several wavelengths and because photopic visibility and visor compatibility are important design criteria the bandpass methods were not developed in detail and efforts were concentrated on the band rejection approach.

The band rejection approach requires that the wavelength to be rejected be specified but has the advantage that the photopic transmission is high because most of the spectrum is not attenuated. It also has the advantage that it can be implemented as a diffraction mirror coating on a pilot's visor thus meeting the need for a true visor protection shield.

3.2 BUGEYE VERSUS VISOR

Of the band-rejection schemes, basically two general types were examined. The first method would incorporate two radiation shields on separate substrates, each of which would be visible to and would protect one

eye only. Such a device could have the form of a "bugeye" visor or a pair of goggles worn inside of a conventional visor. The second method would use a single radiation shield fabricated on a visor, with each point on the visor being designed to simultaneously protect both eyes.

In the design of a diffractional radiation shield, a tradeoff exists between the area of the region to be protected and the distance of the radiation shield from the protected region. Each point on the diffractive surface will adequately shield the design wavelength only over some fixed limited angular range of incident directions. This tradeoff (which is discussed in Section 3.4) is that the closer the diffractive surface is to the protected eye region, the larger becomes the angular range over which adequate shielding must be maintained. This poses difficulties because high angular bandwidths are in practice difficult to attain and are associated with high wavelength bandwidths, which degrade the overall visible transmittance of the shielding surface.

For this reason, the bugeye visor and goggle approaches were rejected. These methods would have required placing the diffractive surface too close to the eye, making the required angular shielding range too great. In order to minimize the angular range, the surface should optimally be placed as far as possible from the eye where it will be visible to both eyes; and therefore must be designed to simultaneously protect both eyes.

The radiation shield placed on a visor thus is chosen over possible bugeye configurations.

3.3 SINGLE VERSUS DOUBLE HOLOGRAM ON VISOR

One method of protecting both eyes with a single diffractional surface would use a single diffraction grating, configured so that light at the design wavelength entering the visor toward one eye would be diffracted away from the visor along the other eye's line-of-sight. By the reciprocity principle, light entering the visor along the second eye's line-of-sight would similarly be diffracted away along the first eye's line-of-sight. Thus, both eyes would be protected by a single diffraction grating.

Furthermore, by making the visor shape an ellipsoid of revolution with the foci positioned at the two eye positions, the holographic fringes in

the diffraction grating would be parallel to the visor surface. For this configuration the holographic grating could be replaced by a multilayer dielectric grating making possible larger bandwidths and higher diffraction efficiencies than could be achieved with diffraction gratings.

One drawback to this approach is that because of the constraint on the visor's shape, the design of the visor can not be optimized to minimize see-through distortion of imagery. Another serious drawback is that the grating's wavelength shielding bandwidth as well as its angular shielding bandwidth would be very wide. For example, to match the characteristics of the test hologram mentioned in the summary, a single grating device (either holographic or multilayer dielectric) having an average refractive index of 1.54 would need to have a wavelength bandwidth greater by a factor of nine than that of the test hologram. Increasing the average refractive index would lower the required wavelength bandwidth of the grating; but even with an average index of 2.5, the necessary wavelength bandwidth would still be 3.4 times that of the holographic device, resulting in much more severe see-through coloration.

Evidently, it is desired to maximize the angular bandwidth of the grating at the design wavelength while simultaneously minimizing its wavelength bandwidth. Two factors determine the angular and wavelength bandwidths of a diffraction grating: its physical properties and its diffraction geometry. The processing methods used in fabricating a holographic diffraction grating determines its physical parameters (grating layer spacing, index of refraction variation, etc.) and may be optimized to maximize the grating's angular bandwidth, but not without also maximizing its wavelength bandwidth. However, for a grating with given physical characteristics, the diffraction geometry can be designed so as to maximize its angular bandwidth while simultaneously minimizing its wavelength bandwidth. This condition is met when light at the design wavelength, which enters the visor along the eye's nominal line of sight, is diffracted away from the visor directly back in the direction of incidence. In order to protect both eyes, two gratings of this type would be used; either in separate layers on the visor, or superimposed as a double exposure inside a single holographic layer. (Figure 3 compares the angular bandwidth for single and double grating shields.)

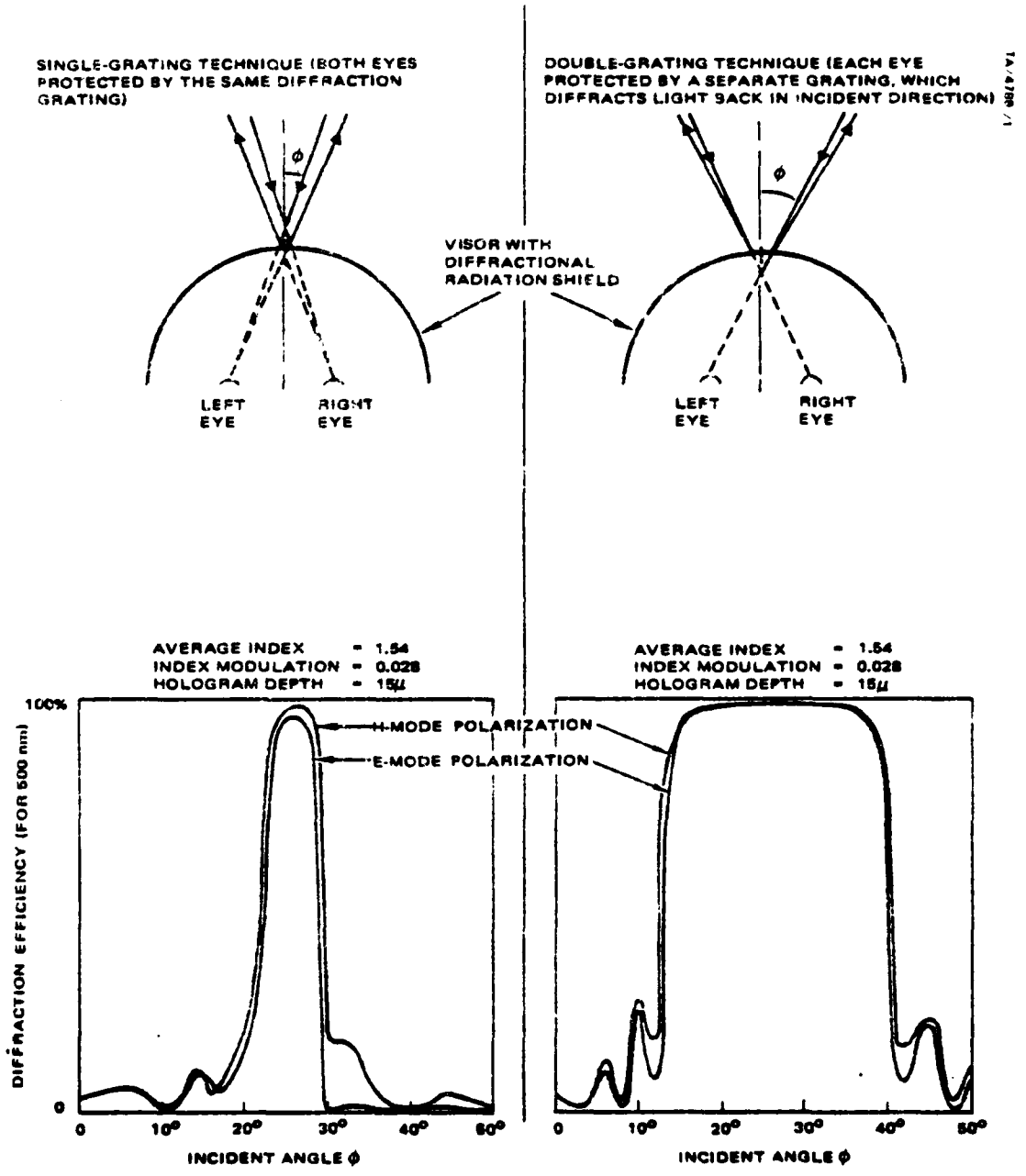

Figure 3. Angular bandwidth comparison: Bandwidth is maximized when rejected light is diffracted directly back in incident direction.

Of all the shielding methods that have been examined, the double grating approach is the most satisfactory. The protective visor would need to be on the order of 70 mm from the eye, and would produce some see-through color variation across the visor, but any other shielding method would either need to have a much wider wavelength bandwidth to maintain the same angular shielding range, resulting in severe degradation of see-through image quality; or else would necessitate placing the diffractive surface much further from the eye in order to compensate for the decreased angular shielding range of the diffraction grating.

3.4 TRADEOFF BETWEEN MAXIMUM PROTECTION ANGLE AND VISOR DISTANCE

Because a diffraction optical reflector operates by Bragg reflection, its rejection efficiency is strongly dependent on angle (Bragg effects are discussed in Section 4). This dependence constrains the design of a visor protection system so that the incoming light angles do not depart too far from the efficient Bragg reflection angle. Figure 4 shows for a particular hologram the variation of diffraction efficiency with angle. The range of angles over which a single point on the holographic shield must reflect incoming light is a function of the size of the protected eye "safe pupil" and the distance from that pupil to the visor as is shown in Figure 5. It is seen that the required visor protection angle can be made smaller by increasing the visor distance or by reducing the size of the protected area. Figure 6 shows a particular visor geometry in which for a 40 mm safe pupil and a 90 mm visor distance the maximum required protection angle is 27°. Other similar diagrams in the appendix Figures A-1 through A-4 show other visor distances and safe pupil sizes. Figures A-5 through A-7 in the appendix graph the protection angles required for each configuration. The combined results of these various configurations are shown on Figure 7 as a tradeoff between visor distance and maximum required protection angle for 20, 30 and 40 mm safe pupil diameters. As an example, one can see that for a hologram that will provide a required amount of rejection over a 30° angle, if a 40 mm safe pupil is required then the visor distance must be 80 mm. To reduce the required visor distance one would need to provide a more efficient and broader hologram or ease the requirements on safe pupil size or rejection value.

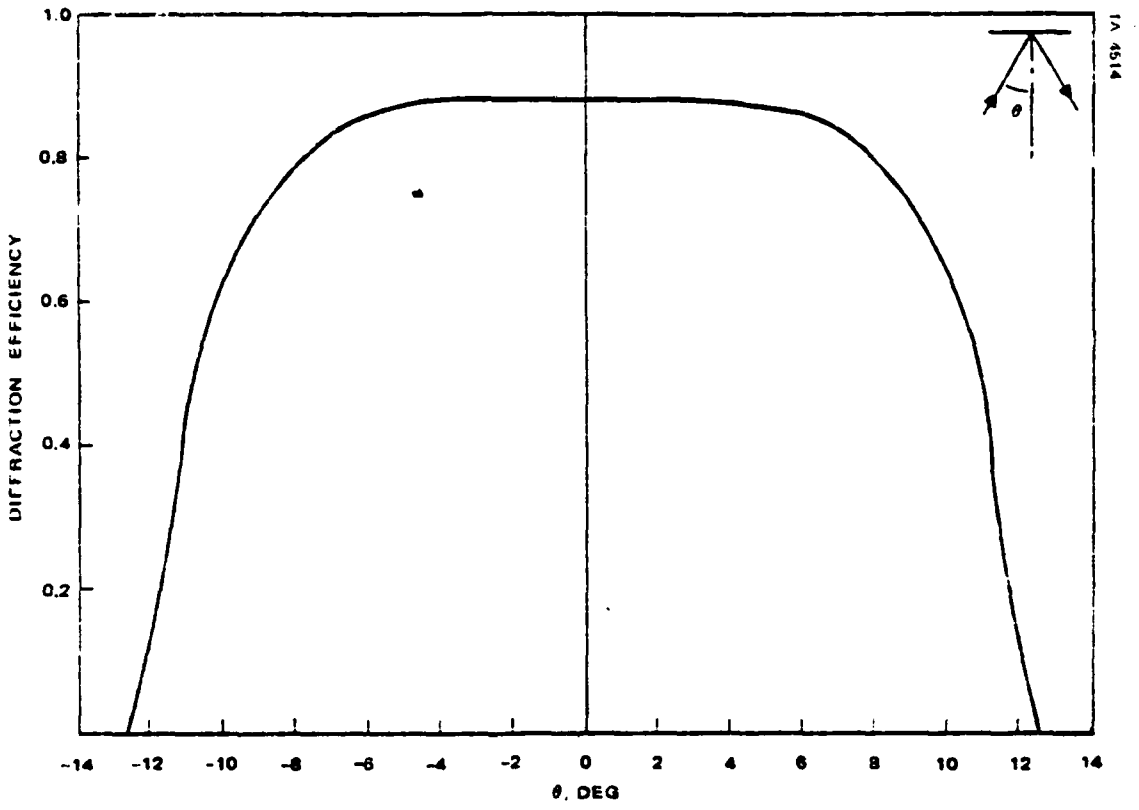

Figure 4. Diffraction lens reflection efficiency versus angular deviation from the construction rays.

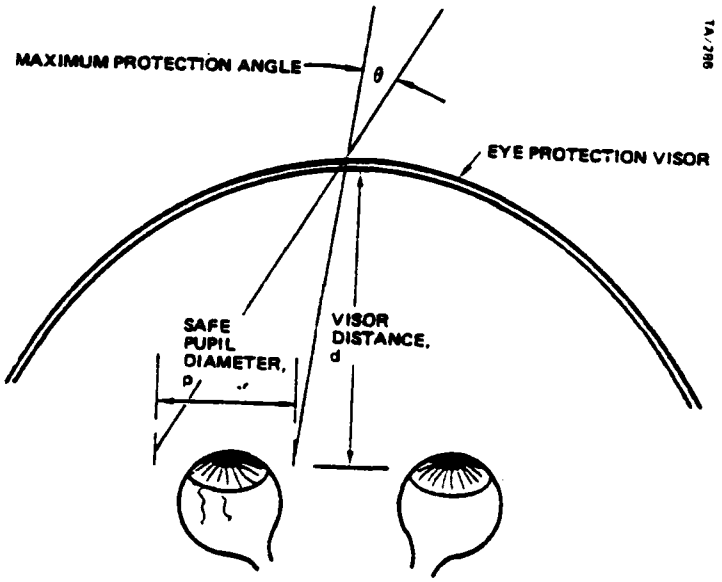

Figure 5. Maximum protection angle required is a function of safe pupil size and visor distance.

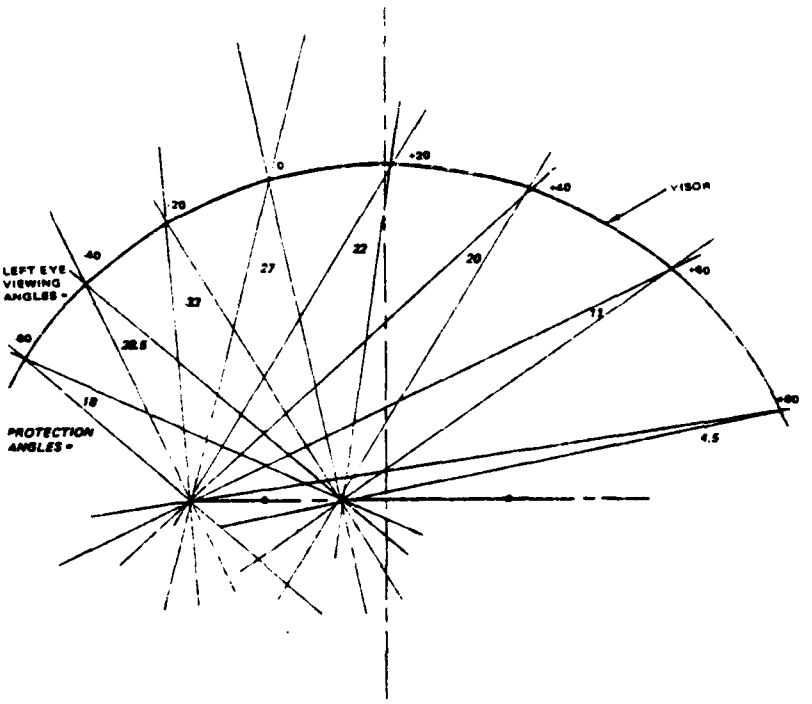

Figure 6. Protection angles for 90 mm visor distance, 40 mm pupil, 115 mm visor radius.

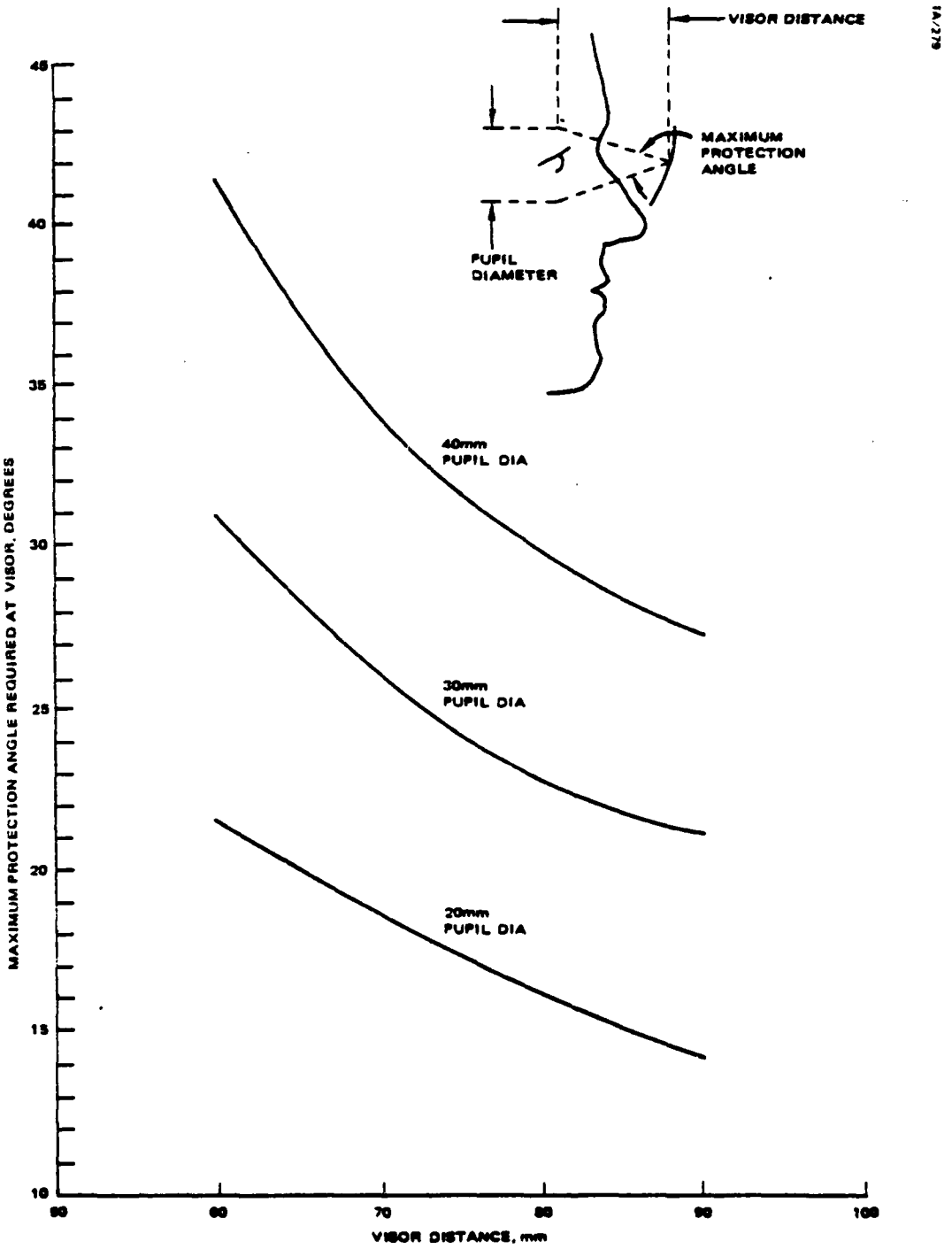

Figure 7. The angular range over which the designated wavelength must be adequately shielded is large when the shielding surface is close to the eye.

3.5 EYE SPACING VARIATION AND VISOR ALIGNMENT CRITERIA

As discussed in section 3.4, the size of the eye pupil to be protected is an important factor which determines the other elements of visor geometry such as minimum visor to eye spacing. The size of the required protection pupil depends on three factors.

1. The basic size of the pupil itself including the effect of eye motion.
2. The variation of inter pupillary distance.
3. The precision of alignment of the visor position.

Typically, a protective visor would need to shield the eye over about a 4 cm diameter region, centered 3 cm from the midpoint between the eyes. This 4 cm figure includes:

- a 2 cm width of the exposed eye region
- about 1 cm to accommodate individual eye positions variation*
- 1 cm horizontal visor positioning tolerance

A visor having an angular shielding range of 30° would need to be placed about 8 cm from the eye in order to shield a 4 cm region of the eye. (See Figure 6.) By reducing the visor positioning tolerance and by making visors in a range of sizes to accommodate different interpupillary distances, the required shielding area could be reduced so that the visor could be brought in closer to the eye. Increasing the visor's angular shielding range would also decrease the required eye-to-visor distance.

*Interpupillary spacing varies among individuals from 50 to 73 mm. (MIL STD 1472 B 5.11.3.13.2)

4.0 SHIELDING HOLOGRAM DESIGN

4.1 POLAR GRAPH DESCRIPTION

The shielding hologram may be described most effectively in the context of a geometrical model known as a reciprocal-space diagram. The diffraction characteristics of any point on the holographic grating are represented on a polar graph (see Figure 8), on which each point represents a specific monochromatic collimated beam of light which passes through the particular point on the hologram with some transmission efficiency. The direction from the polar origin to any given point on the graph represents the collimation direction of the beam inside the grating (related by Snell's Law to its direction outside); and the distance from the origin to the point is equal to the inverse wavelength inside the grating (which is greater by a factor of the refractive index than the inverse wavelength in air). Although the dimensions on the graph represent wavelengths and angles inside the grating, they are for convenience labeled with their air-equivalent values.

Rays that diffract off the grating most strongly are represented on the graph by points that all fall on a straight line; with the position and orientation of the line being determined by the construction geometry and processing used in fabricating the hologram. A contour mapping of diffraction efficiency on the graph will have the form of a narrow ridge peaked over the straight line and falling off rapidly to either side. (Conversely, a contour plot of transmission efficiency will have the form of a straight narrow trough over the line.)

The detailed shape of the diffraction efficiency contour depends on the thickness and the refractive index modulation amplitude of the holographic grating. Increasing the index modulation tends to heighten and broaden the

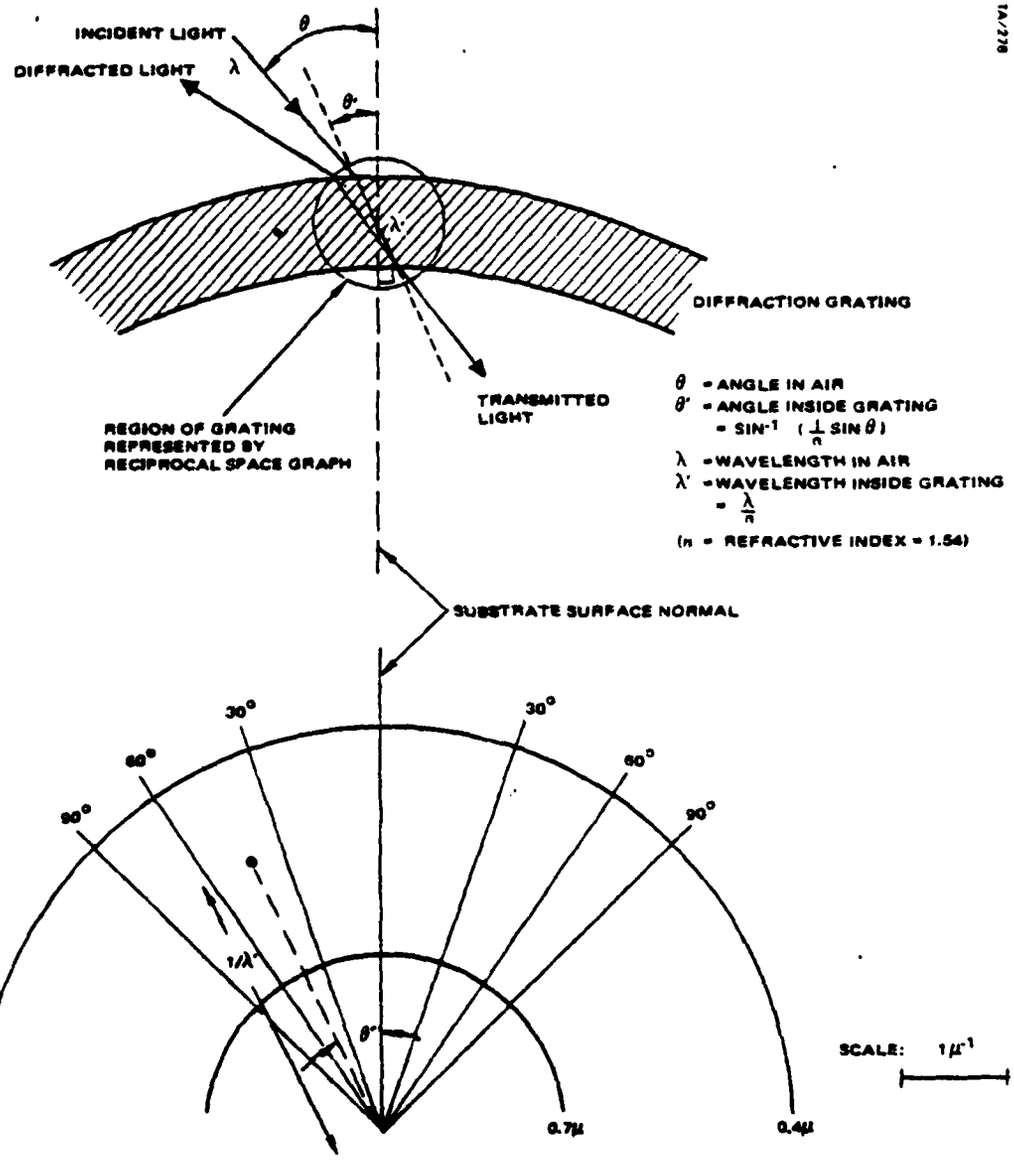

Figure 8. Reciprocal space graph: The graph corresponds to a specific spot on the grating, with each point on the graph representing a particular collimated monochromatic ray of light incident on the spot. Air-equivalent wavelengths and angles are labeled.

ridge. If the index modulation is increased and the grating thickness is decreased by the same factor, the ridge will broaden, but the peak efficiency of the grating will remain unchanged. (Section 4.2 outlines a theoretical method for predicting diffraction efficiencies and computing the direction of the diffracted light.)

Note that if a circle centered at the origin (representing a fan of rays all with the same wavelength) is tangent to the peak efficiency line, the circle will pass very close to the line over a wide angular range near the point of tangency, and hence, the particular wavelength represented by the circle will diffract strongly over a wide angular range. (Although the two dimensional graphs used here only represent the effect of the grating on rays confined to a horizontal plane, a simple three-dimensional generalization may be made. Points in reciprocal space representing a fixed wavelength form a sphere centered at the origin; the points associated with peak diffraction efficiency fall on a flat plane, and both the vertical and horizontal angular bandwidths of the grating for the specific wavelength will be maximized when the peak-efficiency plane is tangent to the constant-wavelength sphere.)

In the context of the shielding hologram, the nominal line of sight is equated with a ray from the origin of the polar graph; and the peak efficiency line of the grating is defined to be tangent to the circle representing the shielded wavelength where the circle crosses the line of sight. (In three dimensions, the peak efficiency plane would be tangent to the shielded wavelength sphere where the sphere intersects the line of sight.) With this configuration the angular bandwidth of the grating will be maximized in the region of the line of sight. By using two such gratings, both eyes may be protected simultaneously.

4.2 DIFFRACTION EQUATIONS

The graphical model discussed in Section 4.1 describes qualitatively the diffraction characteristics of a holographic diffraction grating. The model describes only diffraction efficiencies; no prediction is made of the direction in which light is diffracted by the grating. This section discusses a more complete model which predicts the direction of diffraction and gives

quantitative estimates of the diffraction efficiency. (This model is based on the theory of Kogelnik*.)

The refractive index in a holographic dielectric diffraction grating varies in the form of a periodic plane wave pattern. (See Figure 9.) In performing diffraction calculations, the grating is represented by a vector $\vec{K}$ (the "grating vector") which is directed normal to the fringe planes and has a magnitude equal to the inverse distance between fringe planes. A monochromatic collimated beam of light incident on the grating is represented by its "propagation vector" $\vec{k}_o$, which is directed normal to the wavefronts (in the direction of propagation), and has a magnitude equal to the inverse wavelength. (The wavelength and direction are measured inside the grating, not in air.) The diffracted beam is similarly represented by its propagation vector $\vec{k}_1$, which must have the same magnitude as $\vec{k}_o$, since both beams have the same wavelength.

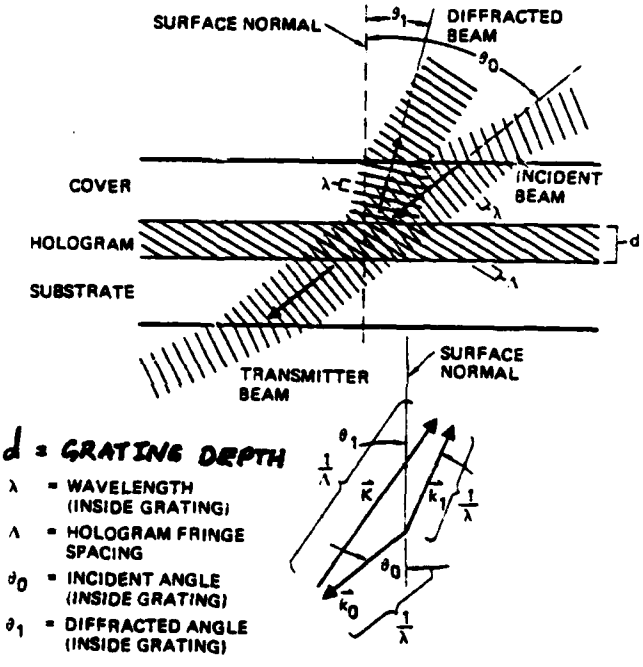

Figure 9. Diffraction grating geometry.

*Bell Sys. Tech J, v. 48, Nov. '69, p. 2909.

The incident beam is said to satisfy the "first order Bragg condition" when the magnitude of the vector $\vec{k}_o + \vec{K}$ is equal to the magnitude of $\vec{k}_o$. (See Figure 10.) In this case $\vec{k}_1$ is equal to $\vec{k}_o + \vec{K}$, and the direction of the diffracted beam is such that the holographic fringe planes may be thought of as mirrors reflecting the incident beam into the diffracted beam. The vectors $\vec{k}_o$ that satisfy the Bragg condition define a line (the "peak line" described in section 4.1), or in three dimensions, a peak plane. The Bragg diffraction efficiency η is given by the formula:

$$\eta = \tanh^2 \left(\frac{\pi d \left(n_1 / n \right)}{\lambda \sqrt{\cos \theta_o \cos \theta_1}} \right)$$

where n_1 is the refractive index modulation amplitude, n is the average refractive index, and λ, d, θ_o, θ_1, are defined in Figure 9.

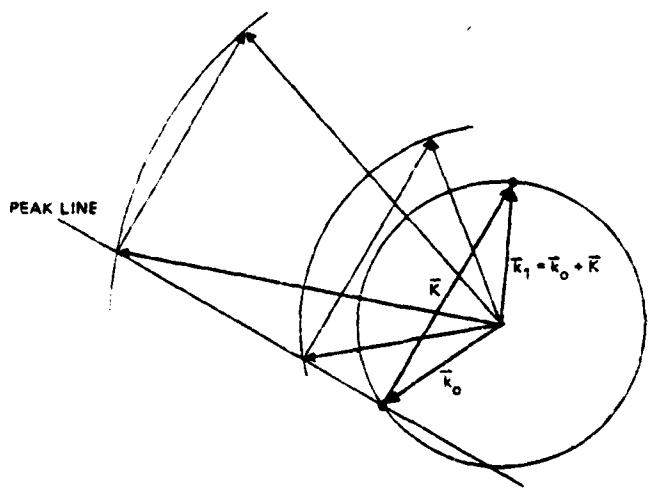

Figure 10. The Bragg condition holds when $|\vec{k}_o + \vec{K}| = |\vec{k}_o|$. The vectors $\vec{k}_o$ that satisfy the Bragg condition define a "peak line" (or a "peak plane" in three dimensions).

When the incident beam deviates from the Bragg condition, diffraction efficiency falls off rapidly and the direction of the diffracted beam can no longer be computed by simply treating the holographic fringe planes as mirrors. The direction of the diffracted propagation vector $\vec{k}_1$ is determined as follows: the component of $\vec{k}_1$ parallel to the hologram substrate surface is equal to the surface component of $\vec{k}_o + \vec{K}$, and the component of $\vec{k}_1$ normal to the surface is such that the magnitude of $\vec{k}_1$ is equal to the magnitude of $\vec{k}_o$. (See Figure 11.) The difference Δ between the component of $\vec{k}_o + \vec{K}$ normal to the hologram surface and the normal component of $\vec{k}_1$ is involved in the diffraction efficiency formula. Diffraction efficiency is maximized when $\Delta = 0$ (the Bragg condition) and falls off rapidly as Δ increases.

Defining:

$$\nu = \frac{\pi d \left(n_1/n\right)}{\lambda\sqrt{\cos\theta_o \cos\theta_1}}$$

$$\epsilon = \pi d \Delta$$

the diffraction efficiency formula is

$$\eta = 1/\left\{ 1 + (1 - \epsilon^2/\nu^2)/\sinh^2\sqrt{\nu^2 - \epsilon^2} \right\}$$

(At the Bragg condition, $\epsilon = 0$ and this formula reduces simply to $\eta = \tanh^2 \nu$.)

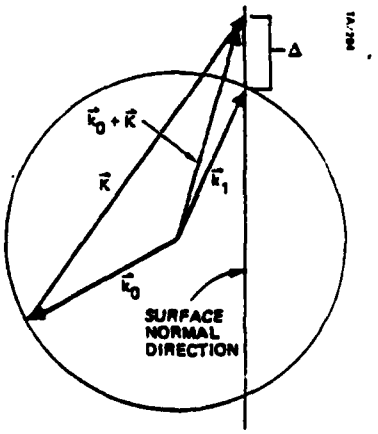

Figure 11. The surface component of $\vec{k}_1$ is equal to that of $\vec{k}_o + \vec{K}$, and the normal component is such that $|\vec{k}_1| = |\vec{k}_o|$.

5.0 CONSTRUCTION OF TEST SAMPLES

5.1 OPTICAL SET UP

Figure 12 shows the optical setup for the fabrication of the test samples. The configuration of the center portion of the visor was chosen for the sample region so that the single exposure apparatus shown could fabricate both left and right eye holograms by rotating either one 180° to form the other.

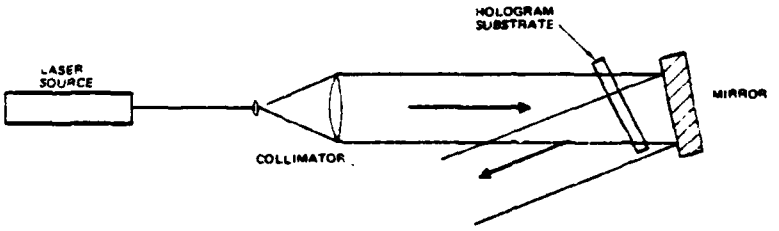

Figure 12. Test sample exposure apparatus.

5.2 HOLOGRAM RECORDING

All hologram recording was done on dichromated gelatin because of its high index modulation and low scatter and loss. The completed sample holograms were sealed with a cover glass and an epoxy layer for protection from abrasion and moisture. For double holograms, one was rotated 180° and the gelatin surfaces of the pair were epoxy sealed together.

6.0 ANALYSIS OF TEST SAMPLES

In order to test the diffraction elements of section 5, a number of small sample holograms were fabricated which simulate the portion of the visor directly in front of and between the eyes. The test samples were designed to shield 0.514u light along a nominal line of sight 26° from the substrate surface normal (in air). The primary objective of the experiment was to determine what shielding efficiencies and angular shielding ranges could be obtained for some wavelength, so no attempt was made to tune the optimally shielded wavelength precisely to the 0.5145 μ design value.

Figure 13 shows a reciprocal space transmission efficiency contour for one of the test samples*. Note that the transmission efficiency is less than 0.1 percent over a large section of the peak line. (From 15° to 40°, transmission on the peak line is between 0.04 percent and 0.05 percent.) Outside of the 50 percentile contour, the transmission increases to a maximum of 78 percent. The intrinsic transmittance of the hologram substrate (which is of green glass, with no anti-reflection coating) is 84 percent, so that transmission efficiency values of over 90 percent outside of the primary diffraction band may be expected of holograms fabricated on good anti-reflection treated substrates.

The effect of the hologram on light at 0.5130 μ demonstrates the kind of shielding efficiencies attainable with such a grating. The 0.5130 μ circle is tangent to the 0.1 percent contour at 26°. To either side of the 26° line, the transmission of 0.5130 μ decreases until it reaches a minimum where

*Figures 13, 14, 15 were generated from data obtained with a Cary-14 scanning spectrometer.

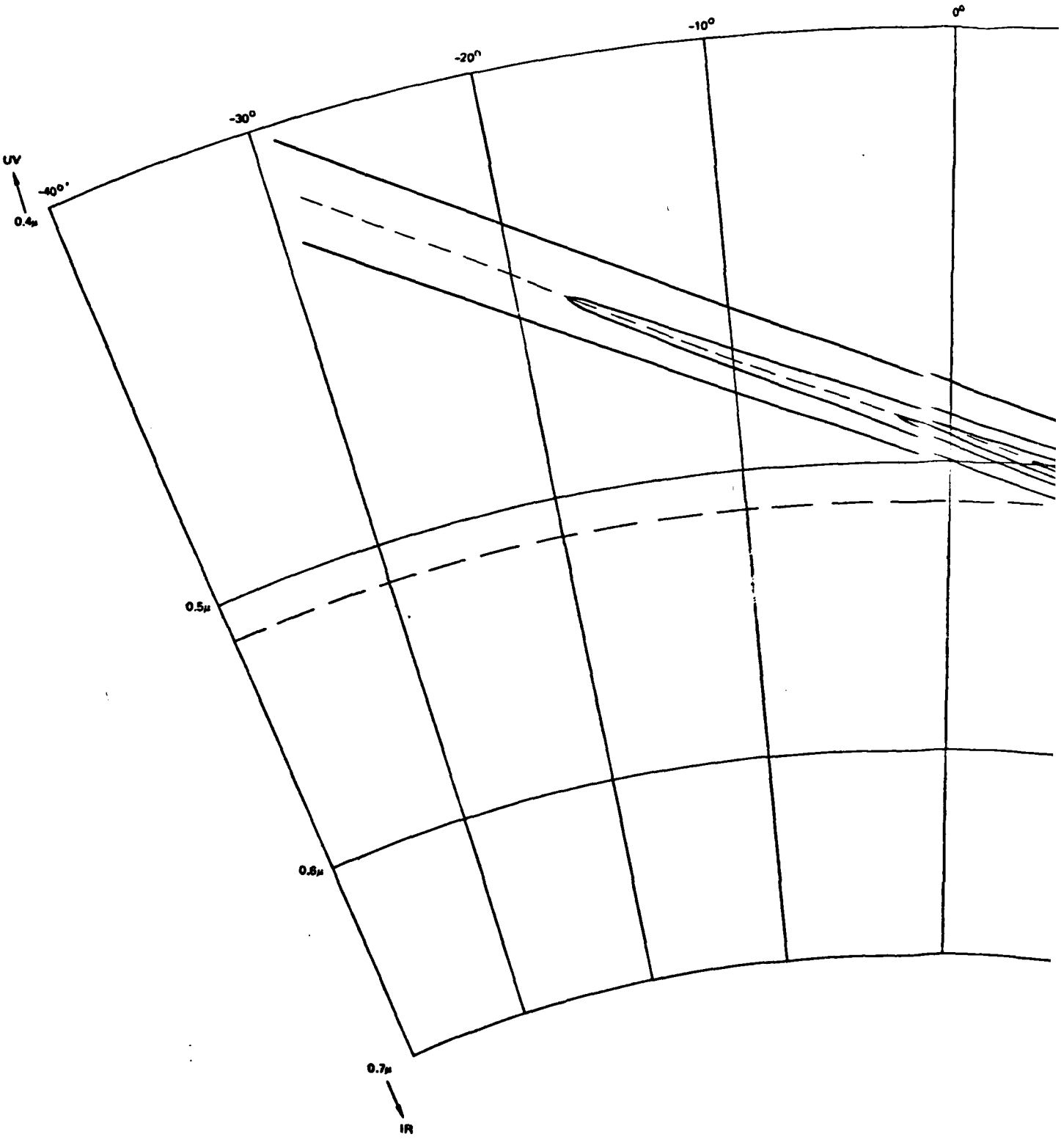
-10°
0°
-20°
-30°
UV
-40°
0.4μ
0.5μ
0.6μ
0.7μ
IR

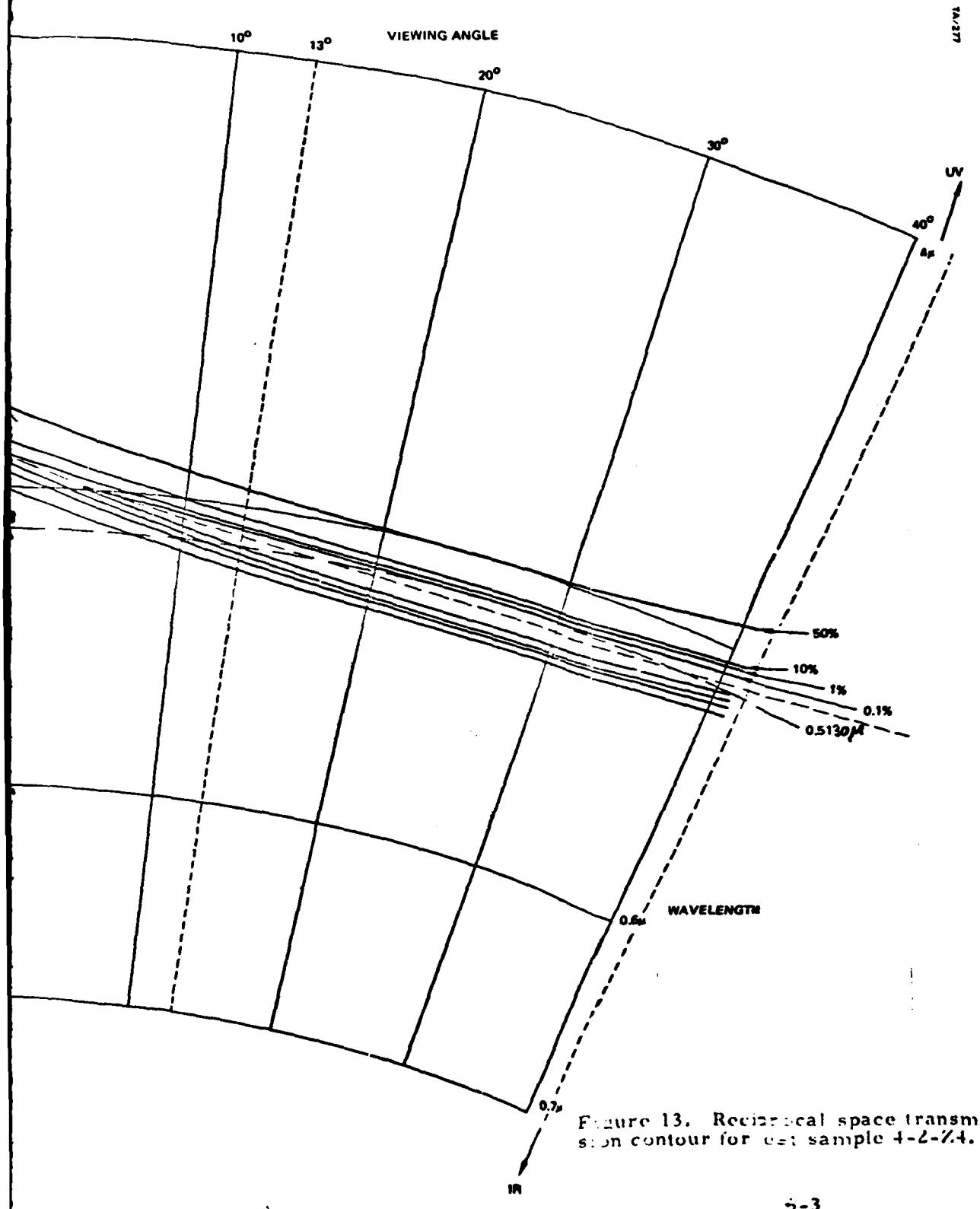

Figure 13. Reciprocal space transmission contour for test sample 4-2-74.

the 0.5130 μ circle crosses the peak line at 17° and at 37°. The circle again intersects the 0.1 percent contour at 13° and at 42°. Thus, the angular transmission spectrum of 0.5130 μ light has the "W" shape illustrated in Figure 14 with transmission not exceeding 0.1 percent between 13° and 42°. (If a correction is made for the 84 percent transmittance of the substrate, the maximum transmittance of 0.5130 μ within the 13° to 42° range would be 0.12 percent instead of 0.1 percent, using a good AR coated substrate.)

Figure 15 demonstrates how two gratings would be combined to protect both eyes. The test sample characterized in the graph consisted of two holograms bonded together in such a way that the design wavelength circle intersects both the left and the right eye's line of sight in the peak efficiency region of one of the two gratings. The shielding hologram for the left eye was one of the poorer quality samples, with its transmission everywhere exceeding 1 percent; but the right eye hologram transmits less than 0.1 percent of 0.5041 μ light over a 24.5° angular range. (Ideally, the transmission contour in Figure 14 would be symmetric about the vertical axis, with both gratings exhibiting the same high shielding efficiency and angular range at the design wavelength.) The photopic transmittance of this double grating is 75 percent; 9 percent of the loss is due to the hologram with 9 percent due to surface reflections and the remaining 7 percent due to absorption in the green glass of the substrate.

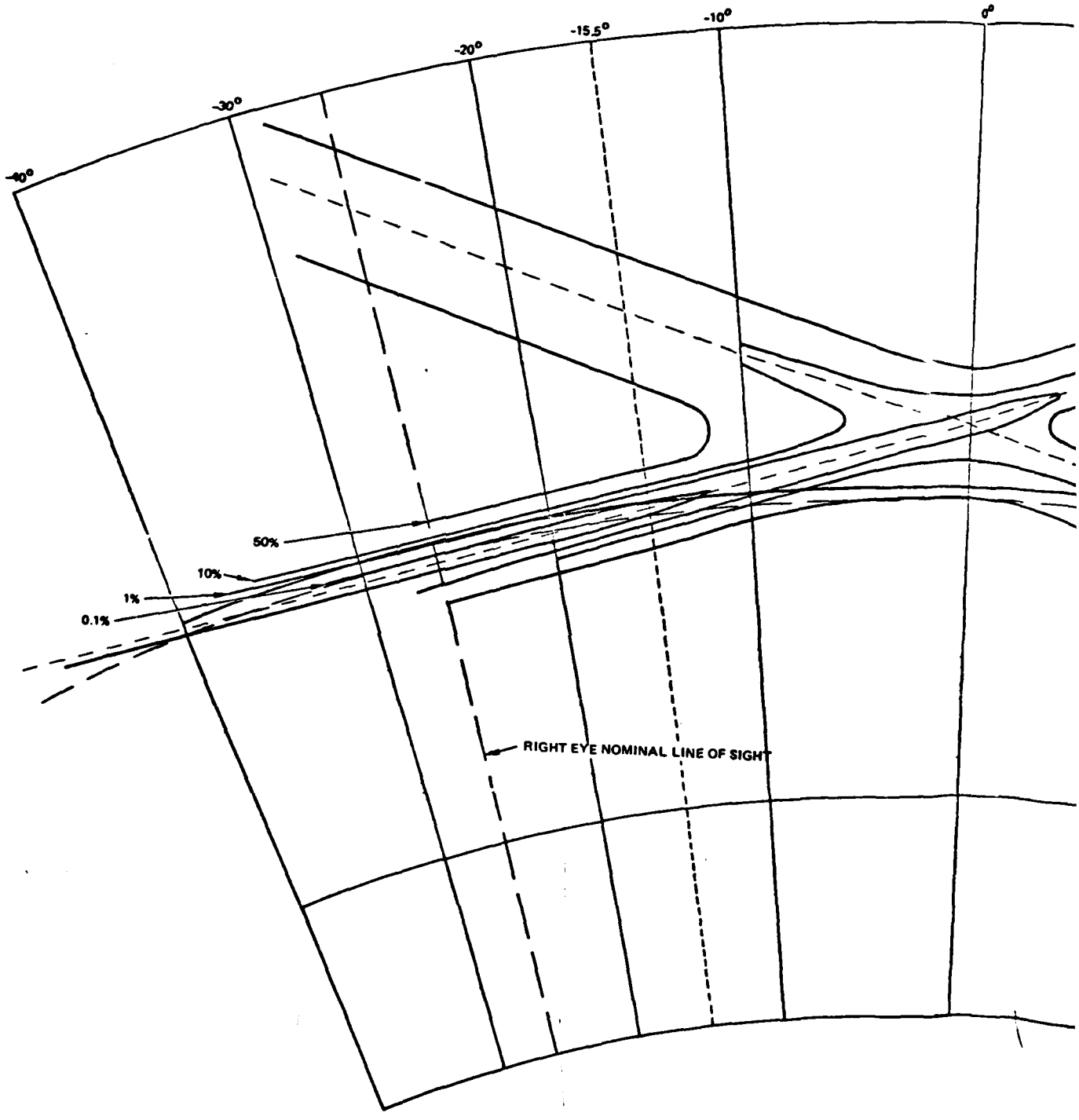
-40°
-30°
-20°
-15.5°
-10°
0°
50%
10%
1%
0.1%
RIGHT EYE NOMINAL LINE OF SIGHT

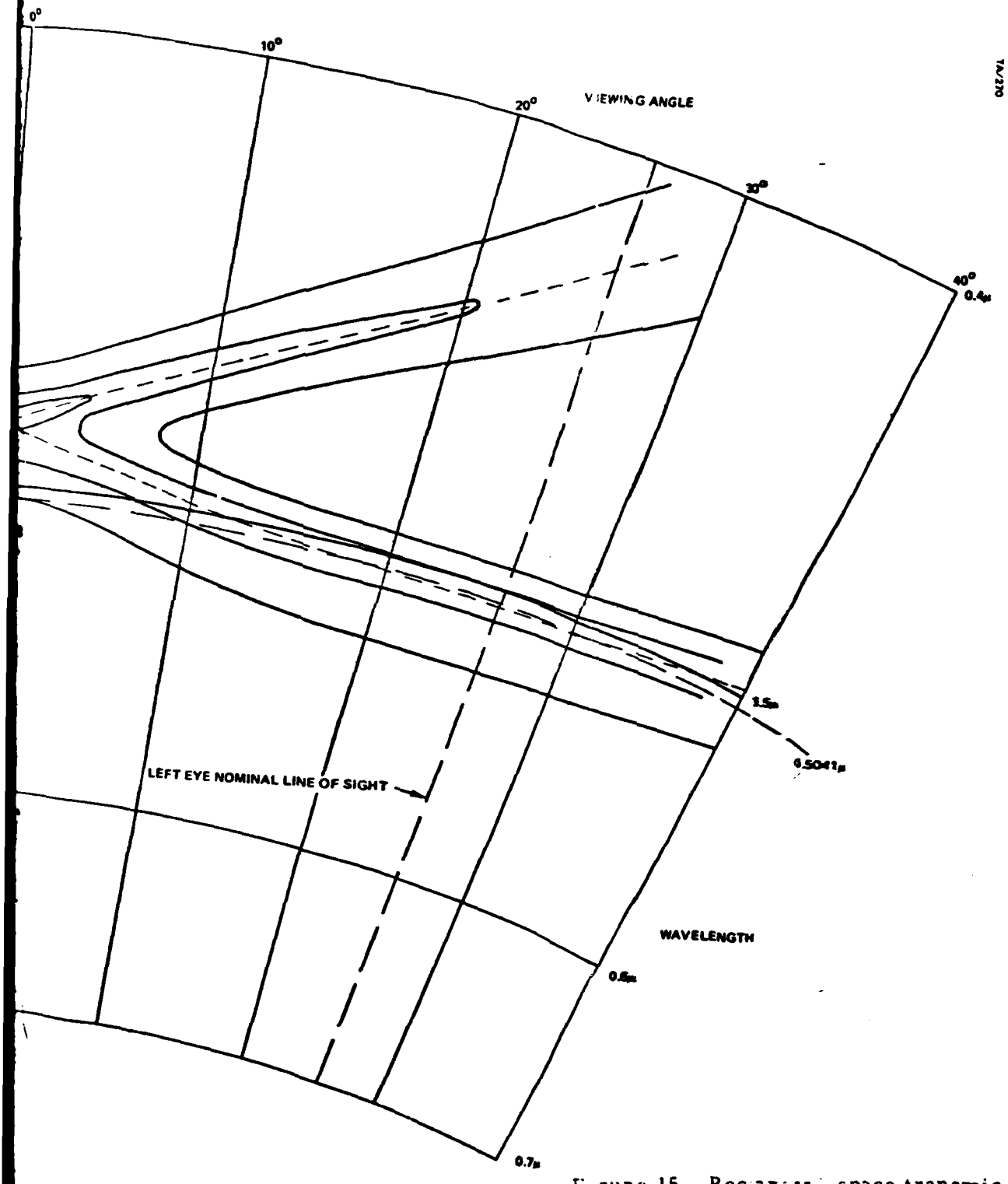

Figure 15. Rectortal space transmission contour for test sample 5 & 6 A3.

7.0 CONCLUSIONS

The sample shielding holograms fabricated for this contract show that one can make a holographic diffraction grating that could be put on a pilot's visor and that would reject 99.9 percent of a specific visible wavelength and still have 90 percent photopic see-through transmission.

The see-through is a main advantage of a holographic grating for this application. This is a result of the narrow rejection bandwidth of the grating when compared to that of dye filters or multilayer dielectric coatings.

A further advantage of a holographic grating over a multilayer dielectric is that a holographic grating can be fabricated on a visor of arbitrary shape. The multilayer dielectric visor shape is constrained because the fringe planes must be parallel to the substrate surface.

While the narrow band characteristics of the diffraction grating offer the foregoing advantages there are also some disadvantages. These were obvious in the discussion of angular selectivity in sections 3.2 and 3.4, which indicated that because the hologram can reject efficiently only over a limited angular range, a diffractive protection visor may need to project out farther from the head or be positioned more precisely than a conventional pilot's visor. Another effect that may be a problem is the variation of see-through coloration with changing look angle through the visor.

A final comment should be made that considerable improvement must be made in process and fabrication control before flyable plastic pilot's visors containing large gratings matching the performance of the small samples of this contract can be fabricated. In particular for these very high efficiency holograms:

- The peak efficiencies and angular bandwidths characterized in Figures 13, 14 and 15 must be repeatably reproduced.

- The wavelength of peak efficiency must be accurately controlled.
- The grating uniformity must be achieved over large areas.
- The wavelength and diffraction efficiency must be made stable.

As these controls are achieved it may be possible to achieve shielding efficiencies greater than the 99.9 percent values obtained in this study. In theory any efficiency less than 100 percent can be obtained without further impairing the photopic see-through of the visor.

APPENDIX A
SELECTED VISOR GEOMETRIES
AND
PROTECTION ANGLE VERSUS VIEWING ANGLE CURVES

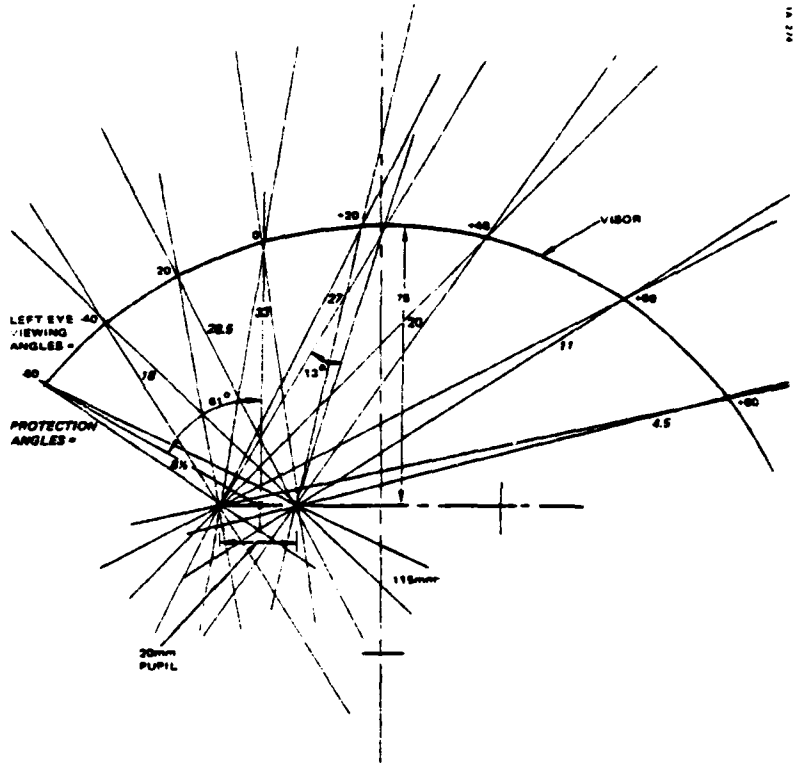

Figure A-1. Protection angles for 20 mm pupil, 75 mm visor distance and 115 mm visor radius.

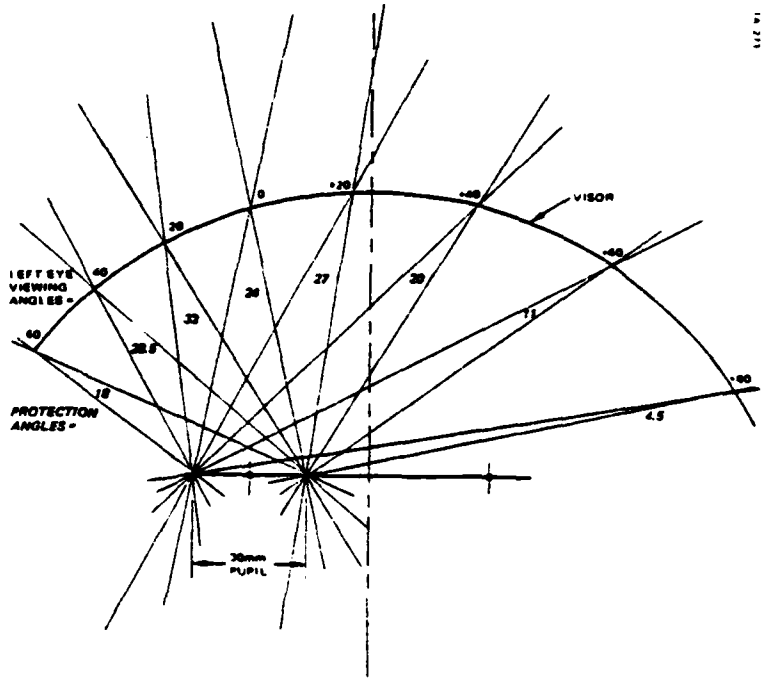

Figure A-2. Protection angles for 30 mm pupil, 75 mm visor distance and 115 mm visor radius.

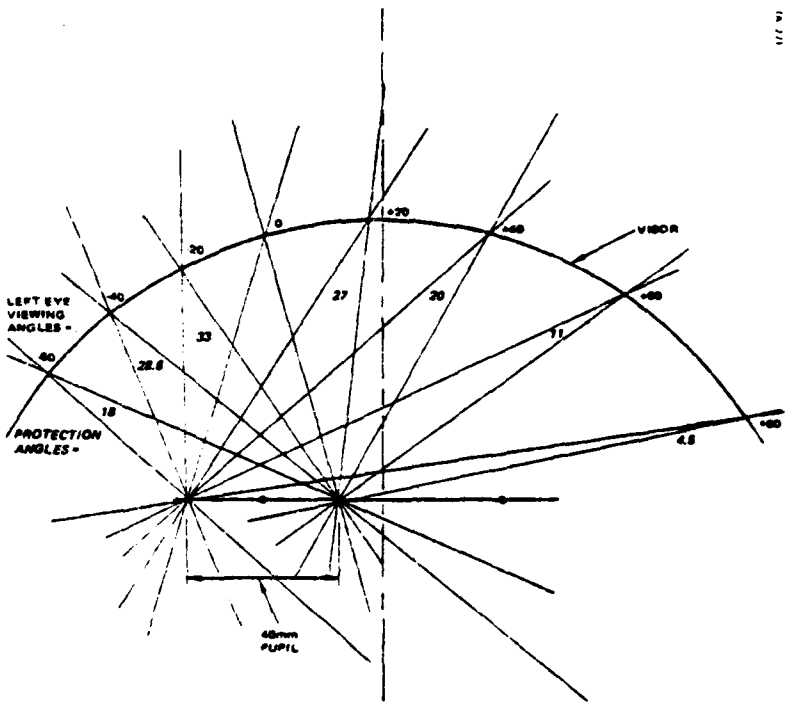

Figure A-3. Protection angles for 40 mm pupil, 75 mm visor distance, and 115 mm visor radius.

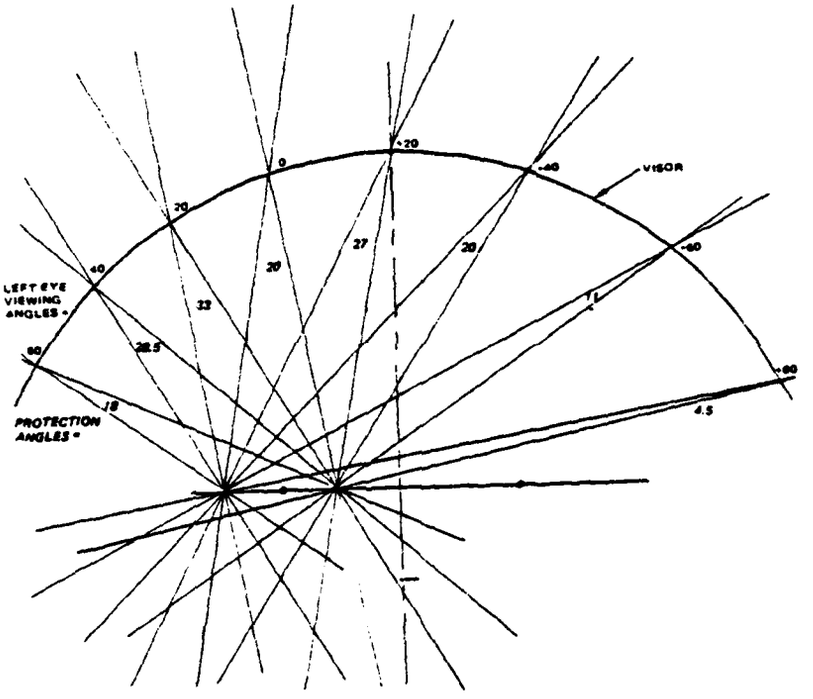

Figure A-4. Protection angles for 30 mm pupil, 90 mm visor distance, and 115 mm visor radius.

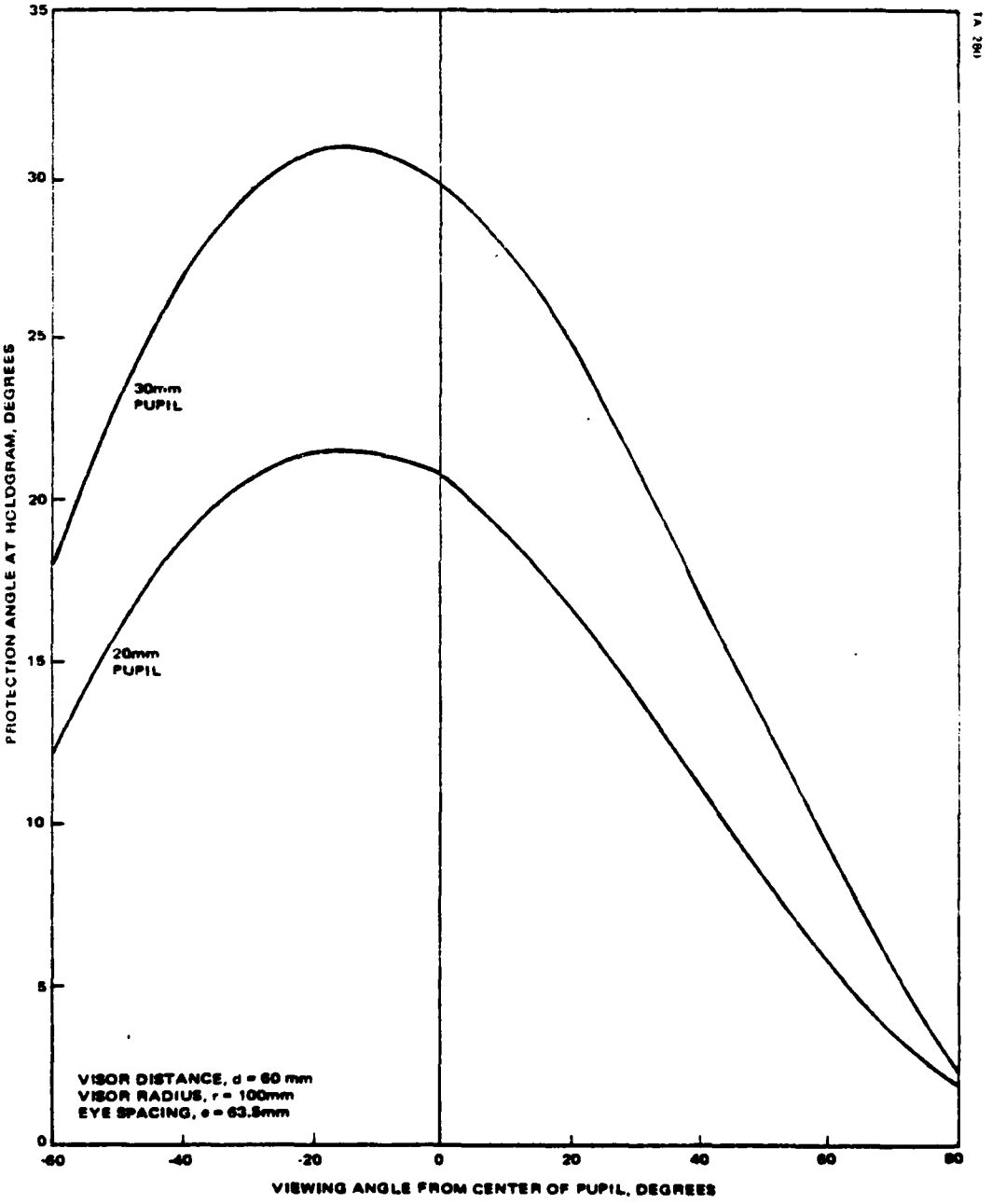

Figure A-5. Protection angle versus viewing angle.

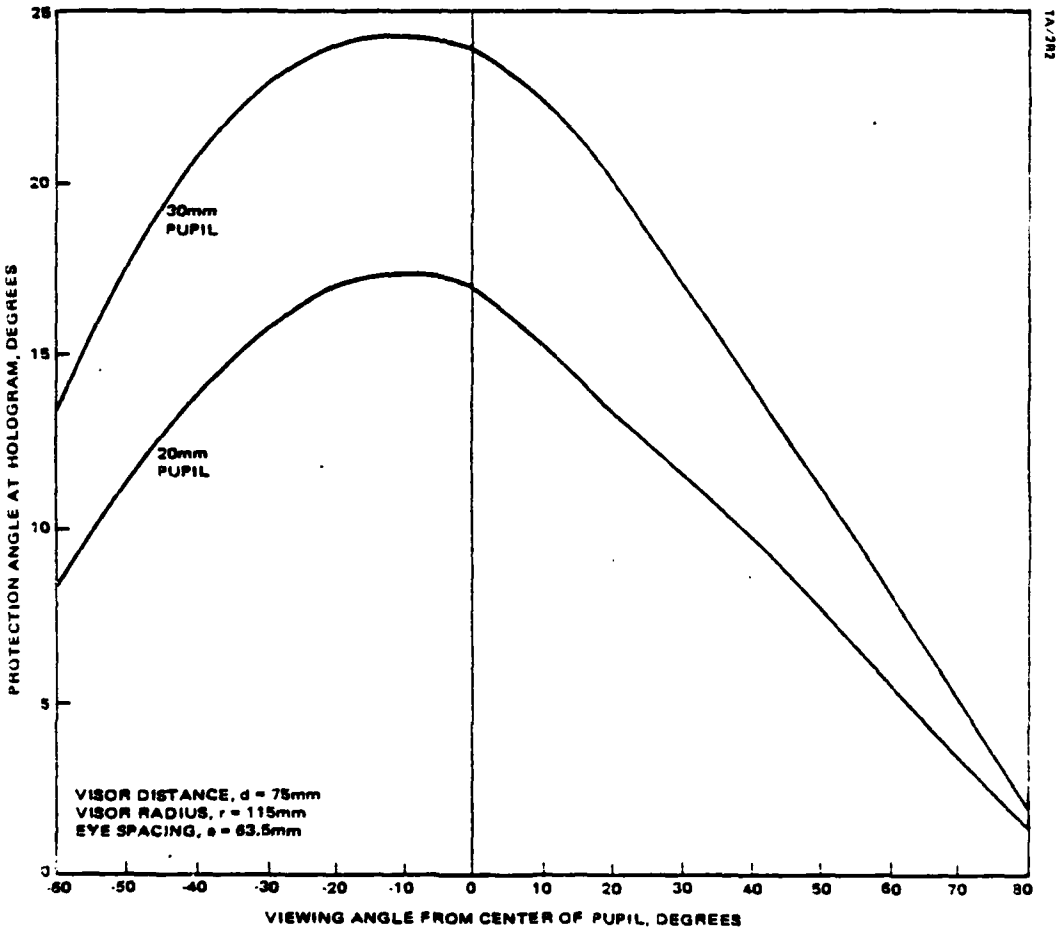

Figure A-6. Protection angle versus viewing angle.

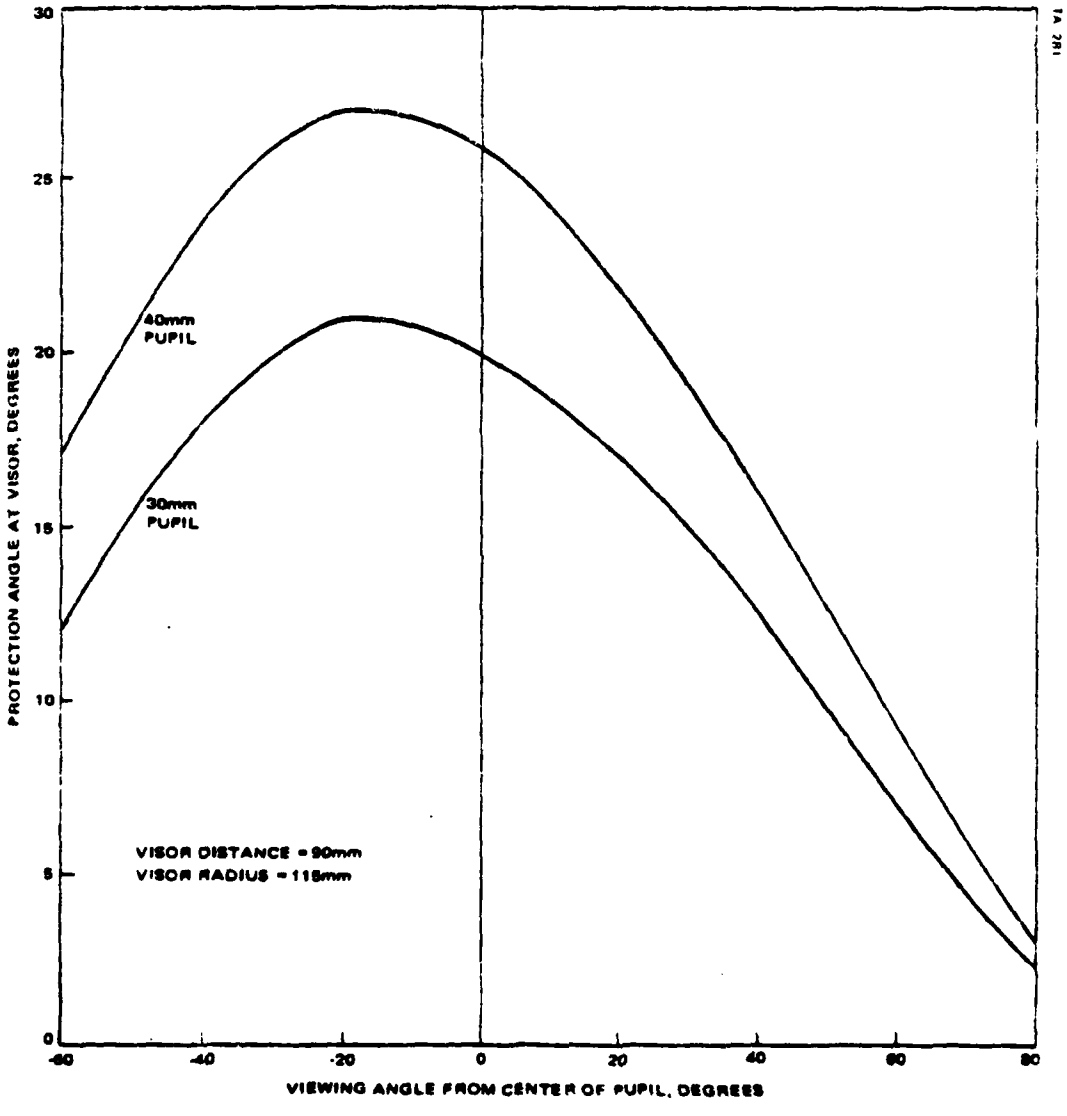

Figure A-7. Protection angle versus viewing angle.

END

DATE
FILMED
4-82

DTIC